

A self-levelling nano-g silicon seismometer

W. T. Pike, A. K. Delahunty, A. Mukherjee, Guangbin
Dou, Huafeng Liu
Department of Electrical and Electronic Engineering
Imperial College London, UK
w.t.pike@imperial.ac.uk

S. Calcutt
Department of Physics, University of Oxford, UK

I. M. Standley
Kinematics Inc.
Pasadena, California, USA

Abstract— We demonstrate a microseismometer with a $2\text{ng}/\text{rtHz}$ noise floor capable of autonomous operation over a wide range of tilts. This represents the highest performance yet achieved by a silicon-based vibration sensor. The microseismometer builds on previous development of a short-period seismometer for NASA's 2016 InSight mission to Mars. The deep-reactive-ion-etched sensor element is unique in that it uses a spring-mass system with a proof mass that moves laterally. This minimizes the damping of the spring mass systems without the need for vacuum encapsulation. The proof-mass position is sensed by a periodic linear capacitive array transducer allowing highly sensitive position detection combined with feedback control at multiple null points. Operation at any of these points enables the sensor to function over a large tilt range without compromising the noise performance. As well as the capacitive sensing elements, the proof mass has planar coils on the surface to electromagnetic actuator when placed in a static magnetic field. The MEMS sensor element is connected to an electronics feedback circuit similar to those used in broad-band seismometers allowing the sensor to act as a velocity output force balance transducer.

Keywords—accelerometer, DRIE, capacitive transducer, seismometer

I. INTRODUCTION

The general operating principle of a seismometer is the sensing of the displacement of a suspended proof mass from its undisturbed position as a result of an external seismic acceleration [1]. All high-resolution seismometers have to measure these low-level seismic signals against the background of the constant gravitational field, a difference of up to eight orders of magnitude [2]. This normally necessitates careful leveling of the sensing element to less than a degree of the gravitational vector to both ensure that the dynamic range of the output is not compromised by a large offset and that the mechanical alignment is maintained with known cross-axis forces. This alignment produces the small gap between the plates of a sensing capacitive transducer, with the capacitive gain inversely proportional to the gap.

Controlling the tilt of a seismometer is generally achieved by a combination of initial crude leveling by hand followed by more precise automated leveling using stepper-motor actuation. Such an approach presents a challenge to installing

This work has been supported by the UK Space Agency as a contribution to NASA's InSight 2016 mission to Mars.

seismometers in extreme environments where human intervention is impossible, such as planetary deployments or volcanic eruptions. In addition the mechanical leveling mechanisms require additional resources which can be comparable or greater than the seismometer itself.

This work describes a microseismometer that has been developed for planetary deployment, with the requirements of autonomous operation under a range of deployment tilts ($\pm 20^\circ$), robustness to shock and vibration (up to 1000 g), operation over a wide range of temperatures (-80C to 40C), all within a limited power ($< 120\text{ mW}/\text{axis}$) and mass ($< 40\text{ g}/\text{sensor}$). As the seismic activity of Mars is expected to be very low, high sensitivity at the $\text{ng}/\sqrt{\text{Hz}}$ level is also a requirement. Meeting these requirements opens up novel applications in terrestrial seismic sensing.

II. APPROACH

We have adopted micromachining of single-crystal silicon by through-wafer deep reactive-ion etching to produce a suspension to meet these requirements [3]. The geometry of the lateral suspension has been selected [4] to produce a fundamental vibrational mode in the plane of the wafer of between 6 and 12 Hz with maximum cross-axis stiffness in a 20 to 25mm die.

The motion of the proof mass is sensed capacitively between an array of parallel electrodes on the proof mass and a matching fixed array on a strip separated by a fixed gap from the proof mass, a variant on the scheme used most commonly in electronic micrometers [5]. As the proof mass moves, these two arrays move in and out of registry, with the capacitance varying with their mutual overlap. In contrast to the more usual arrangement in which the gap between the electrode changes, such a geometry produces a periodic output with the range determined by the maximum lateral motion of the proof mass, and the period by the periodicity of the electrodes. The output gain is maximized by using two sets of moving electrodes on the proof mass excited with out-of phase sinusoidal voltages and differentially amplifying the voltage between two sets of fixed electrodes. The overall gain is set by the driving voltage and the ratio of the capacitance between the drive and sensing electrodes and the sum of the stray capacitance between the sensing electrodes and the input capacitance of the differential amplifier.

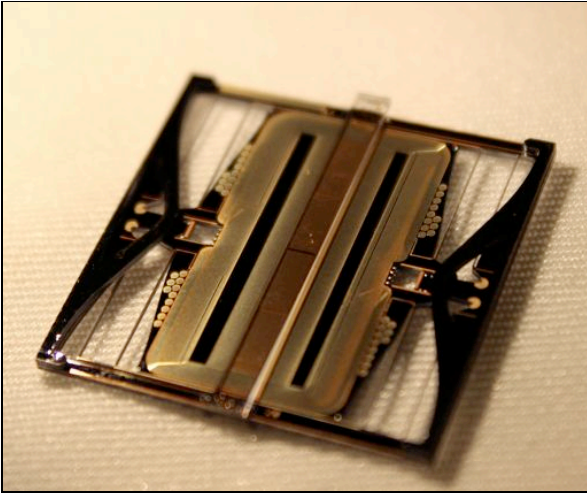


Fig. 1. The 25-mm packaged sensor with the central proof mass between the suspensions on either side. The glass strip with the fixed electrodes is bonded across the center. Additional silicon structures on the left and right of the frame provide shock protection.

As the capacitive transducer produces a periodic signal, every second zero crossings in the output can be used as null point for a control loop with suitable actuation to move the proof mass. We use an electromagnetic actuator to produce a lateral force on the proof mass in the compliant direction of the suspension: a series of conductive coils on the proof mass encircle the electrode array while an out-of-plane magnetic field is produced by magnetic circuit around the die. The actuator has sufficient strength to maintain the position of the proof mass about a single null point for displacements a little more than the period of the capacitive transducer. For larger motions the feedback is unable to maintain control and the proof mass moves to the adjacent null point. Such a motion in general will correspond to a change in the sensor rather than a seismic signal.

When the sensor is powered up, the feedback initially uses a short integration time constant to drive to the nearest null point which will depend on the tilt of the sensor and after stabilization switches to a longer time constant corresponding to control the mass position while a second, faster, control loop

maintains the proof mass at the null point producing a velocity output.

The overall performance of the microseismometer in terms of the smallest seismic signal that can be detected is determined by the self noise of the sensor. This noise is the sum of contributions from the electronics and the motion of the proof mass induced thermodynamically by any damping according to the fluctuation-dissipation theorem [6]. The electronics contribution in turn is set by the input noise of the preamplifier divided by the product of the mechanical transfer function of the suspension and displacement gain of the capacitive transducer.

Vacuum encapsulation of the sensor provides a way to remove the thermodynamic noise, but requires increased packaging costs and considerable reliability testing. We have chosen to select the geometry of the design to minimize this noise contribution without evacuation, reducing its level to the electronics noise.

The thermodynamic noise is given by the ratio of kinetic energy due to free oscillation divided by the energy lost in any one oscillation and is dominated by Couette flow of gas in the gap between the fixed and moving plates of the capacitive transducer. The mechanical transfer function depends on the resonant frequency of the suspension, with the larger gains from a lower frequency requiring a longer suspension and larger proof mass and hence larger die. The suspension also has to be able to accommodate the motion of the proof mass due to tilt. For a given die size, minimization of the noise amounts to a trade between the damping and the displacement gain of the transducer. There are two governing geometrical parameters: the first is the area of the capacitors which increase the transducer displacement gain in proportion to the ratio of the sensor-to-stray capacitances but in turn proportionately increases the damping; the second is the gap between the fixed and moving capacitors with the displacement gain and the damping both in inverse proportion to the size of the gap.

The design of the microseismometer seeks to optimize this trade by restricting the area with the minimum gap for gas flow a thin strip dedicated to displacement transducer rather than the using a glass die of the same size as the silicon as used in our previous designs [7]

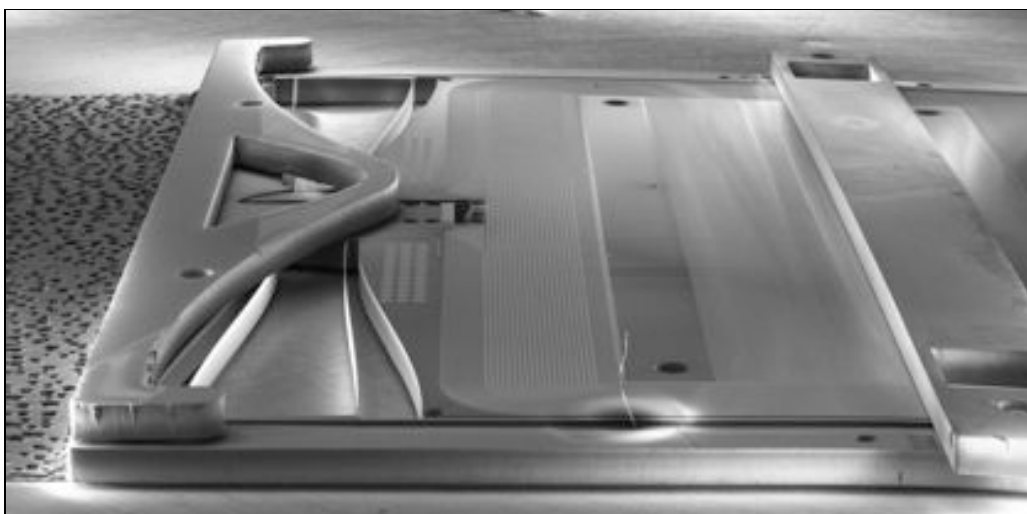


Fig. 2: Oblique view of one half of the 25-mm sensor showing one set of suspension springs and the displacement transducer strip across the center of the proof mass.

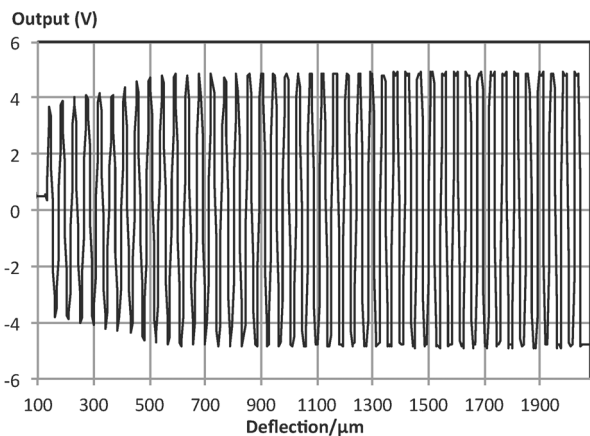


Fig. 3: Output of the displacement transducer across the full range of motion of the proof mass corresponding to a 30° tilt range

III. FABRICATION

Fabrication of the coils and suitable shielding for the drive electrodes on the proof mass requires two metallization layers on the proof-mass wafer separated by an insulator on a silicon wafer. A thermal oxide is grown on the $525\text{-}\mu\text{m}$ thick Si wafer. The first metal layer is produced by 300 nm of sputtered gold, lithographically patterned and wet etched. The insulator is $1\text{ }\mu\text{m}$ of silicon oxide deposited by plasma-enhanced chemical-vapor deposition (PECVD), lithographically patterned and dry reactively-ion etched to open windows to the underlying sputtered first metal layer. A second metal layer is formed by electroplating $4\text{ }\mu\text{m}$ of gold on a sputtered gold seed layer in a lithographically patterned mold. After plating is completed, the mold is removed by dry etching and the unplated seed layer by a wet etch.

The DRIE to produce the overall suspension uses lithographically patterned resist, and the initial removal of the PECVD and thermal oxide by RIE. The through-wafer DRIE is achieved into two steps, with a backing wafer mounted in the second step prior to breakthrough and a backside aluminum layer to minimize footing damage as the etch completes. After the etch the resist is removed and the dies are singulated by breaking a series of tabs that bridge DRIE channels separating the dies.

The fixed electrodes of the displacement transducer are fabricated by electroplating $4\text{ }\mu\text{m}$ of gold on a glass wafer using the same process as on the silicon wafer. The glass wafer is then diced into strips 2-mm wide and 27 mm long for mounting across the center of the proof-mass dies. The strip is bonded to the proof-mass die using AuSn solder balls. $100\text{-}\mu\text{m}$ diameter solder balls are first reflowed onto pads on the glass strips. The volume of the solder ball and the area of the pads determines the $12\text{-}\mu\text{m}$ gap between the fixed and moving electrodes. The strips are positioned on the proof-mass dies for a secondary reflow onto corresponding pads on the frame. The solder provides the electrical connections to a series of pads at one end of the strip.

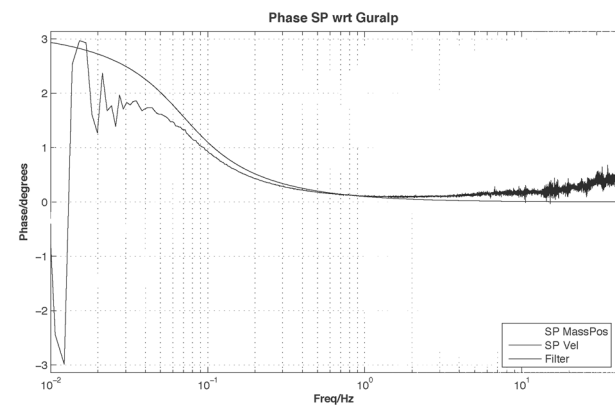
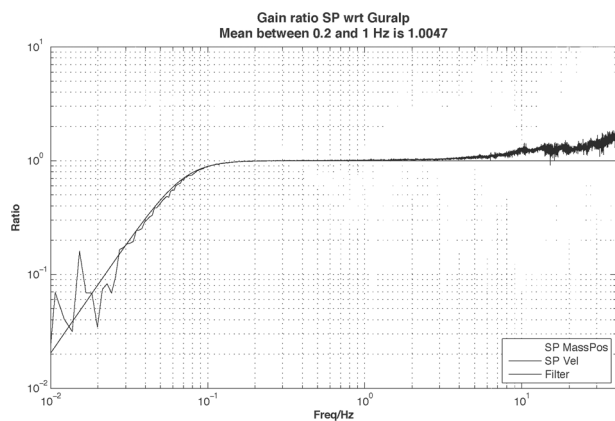


Fig. 4: The amplitude and phase of the velocity response of the microseismometer determined with reference to a conventional velocity-

With a further reflow, additional silicon structures are bonded to the frame to limit motion on the out-of-plane direction and so prevent damage to the suspension from vibration and shock. Further lower-temperature reflow of silver-tin-copper solder balls in pockets formed by the DRIE provide shock protection for motion in the plane of the die [8].

The packaged sensor is mounted within the magnetic circuit. Wire bonds from the pads on the glass strip connect to an electronics board containing the preamplifier. The sensor, magnetic circuit and preamplifier electronics are enclosed in a hermetically sealed box and connected to external electronics that provide the feedback and output signals.

IV. RESULTS

To demonstrate the extended range of the microseismometer, one of the electromagnetic actuation coils can move the proof mass across the entire tilt range. If feedback is not engaged, the displacement transducer will produce an output with the periodicity of the capacitive geometry. Fig. 3 shows the output from the displacement transducer with a period of $48\text{ }\mu\text{m}$. As the deflection is increased, the gap between the plates decreases, and this is evident at the lowest values of deflection as a reduced amplitude in the signal. Modelling of the output indicates that over the entire displacement range of 2 mm the proof mass

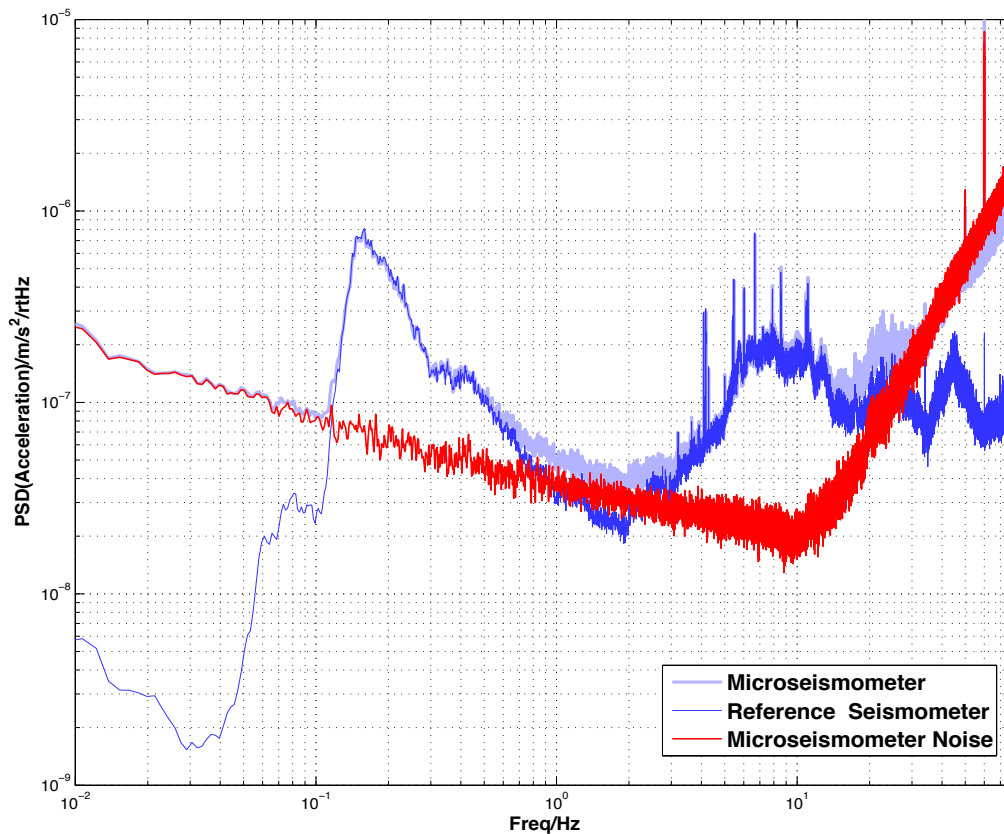


Fig. 5: Ambient seismicity acceleration noise spectral density determined by the conventional seismometer and microseismometer and the derived self noise of the microseismometer.

moves 4 μm towards the glass strip. With the feedback engaged, the microseismometer can operate stably at any of the null points of the fig. 3 with a positive slope. The slope of this output voltage with displacement gives the gain of the transducer in V/m, determining the contribution to the noise from the preamplifier.

The transfer function of the microseismometer output was verified by comparison to a conventional seismometer's velocity output. Fig. 4 shows the amplitude and phase, illustrating the expected roll off in the response at low frequencies but with a velocity output above a frequency of 0.1 Hz.

Coherence between the output of the two seismometers gives a measurement of the microseismometer noise under the assumption that the microseismometer is the cause of any loss in coherency [9]. Fig. 5 shows the acceleration spectral density of the reference seismometer and the microseismometer, in this case with an 11 Hz suspension. The noise rises with a slope of 1/2 with decreasing frequency due to the flicker noise of the preamplifier. Above the resonant frequency of the suspension, the noise rises with a slope of 2 due to the transfer function of the suspension.

At the crossover close to the resonant frequency of the suspension the derived self noise of the microseismometer falls below $2 \text{ ng}/\sqrt{\text{Hz}}$ at its lowest point.

V. CONCLUSIONS

We have demonstrated a microseismometer with a $2 \text{ ng}/\sqrt{\text{Hz}}$ noise floor capable of autonomous operation over a wide range of tilts. This represents the highest performance yet achieved by a silicon-based vibration sensor.

- [1] E. Wietlandt and G. Streckeisen "The leaf-spring seismometer: Design and performance" *Bull. Seis. Soc. America* Vol. 72 pp 2349-2367, 1982
- [2] J. Petersen "Observations and Modeling of Seismic Background Noise" U. S. Geol. Survey Open-File Report 93-322, 1993
- [3] W. T. Pike, W. J. Karl, S. Kumar, S. Vijendran and T. Semple "Analysis of sidewall quality in through-wafer deep reactive-ion etching," *Microelectronic Engineering* Vol. 73-74 pp 340-345, 2003
- [4] W. T. Pike and S. Kumar, "Improved design of micromachined lateral suspensions using intermediate frames," *J. Micromech. MicroEng.* Vol. 17 pp 1680-1694, 2007
- [5] L. K. Baxter "Capacitive Sensors" Ann Arbor, IEEE, 2000
- [6] T. B. Gabrielson "Fundamental Noise Limits for Miniature Acoustic and Vibration Sensors" *J. Vibration and Acoustics* Vol. 117 pp405-410, 1995
- [7] W. T. Pike, I. M. Standley and S. Calcutt "A Silicon Microseismometer For Mars" *Proc. 17th Transducers Conf., Barcelona, Spain, June 16-20, Paper M4A.006*, 2013
- [8] A. K. Delahunty and W. T. Pike "Metal-armouring for shock protection of MEMS", *Sensors and Actuators A*, Vol. 215 pp36-43, 2014
- [9] A. Barzilai, T. VanZandt, T. Kenny, "Technique for measurement of the noise of a sensor in the presence of large background signals", *Rev. Sci. Instr.* Vol. 69 pp 2767-2772, 1998